



Cause Analysis of Whole Vehicle NVH Performance Degradation under Idle Conditions



Haiping Lai¹, Huaguang Xu¹, Nian Liu¹, Jieliang Guo¹, Ruiqiang Zhang², Haigang Wei^{1*}

¹ GAC MOTOR Co, Ltd, 511434 Guangzhou, China

² College of Automotive Engineering, Jilin University, 130022 Changchun, China

* Correspondence: Haigang Wei (weihg@gacmotor.com)

Received: 11-28-2023

Revised: 01-02-2024

Accepted: 01-12-2024

Citation: H. P. Lai, H. G. Xu, N. Liu, J. L. Guo, R. Q. Zhang, and H. G. Wei, "Cause analysis of whole vehicle NVH performance degradation under idle conditions," *Mechatron. Intell Transp. Syst.*, vol. 3, no. 1, pp. 1–15, 2024. <https://doi.org/10.56578/mits030101>.



© 2024 by the authors. Published by Acadlore Publishing Services Limited, Hong Kong. This article is available for free download and can be reused and cited, provided that the original published version is credited, under the CC BY 4.0 license.

Abstract: The NVH (noise, vibration, harshness) performance of automobiles is a key issue in enhancing user comfort. However, car manufacturers and original equipment manufacturers often invest more research and development effort into the new car performance at the initial design stage, neglecting the study of whole vehicle NVH durability and reliability, and this can significantly affect the user's riding experience. This paper focuses on the phenomenon of NVH performance degradation under idle conditions. Using LMS data acquisition equipment and software, vibration acceleration and frequency at 17 points on the vehicle, including the steering wheel, seat rail, and engine mount, were collected and analyzed. By conducting comparative experiments, the causes of NVH performance degradation after long mileage were explored. This aims to provide new ideas for improving the durability and reliability of whole vehicle NVH in future research and production.

Keywords: Automotive NVH; Idle condition; Performance degradation

1 Introduction

With the rapid development of the automobile industry, people's requirements for the riding comfort of cars have been increasing. In this context, the NVH (noise, vibration, harshness) performance of automobiles has become an important evaluation indicator and has seen significant development in recent years. A market survey on the quality level of vehicles in use found that the NVH performance of some vehicles shows a noticeable deterioration after driving 50,000 to 100,000 kilometers. In particular, the degradation of vibration under idle conditions is one of the issues that receive many complaints in the market.

Usually, at low-speed conditions such as startup and idle, the powertrain generates low-frequency, high-amplitude vibrations, leading to significant in-vehicle vibrations that affect the overall NVH performance and reduce riding comfort. Various car manufacturers and scholars have been committed to seeking optimization methods. Timpner F. F. of General Motors, believes that the improvement of NVH performance can rely on the optimization of the suspension system. He proposed calculation methods for the strike center, torque axis, and elastic center based on the theory and computational methods of six-degree-of-freedom decoupling, which are used for suspension matching design. B. L. Belten-Knight utilized the principle of the impact center and considered positioning the suspension points near the elastic vibration nodes to achieve better vibration isolation effects. However, designers often only consider the performance of new vehicles and neglect the aging and performance degradation of the suspension system due to prolonged use and driving, and this can lead to changes in the natural frequencies of various system modes and a decrease in the decoupling degree of vibration modes. This study aims to explore the causes of the degradation of the whole vehicle NVH performance, providing new ideas for research and optimization.

This study analyzes two main two sources of vibration excitation at the whole vehicle level: first, the road excitation at the wheels caused by road unevenness during driving, and second, the vibration excitation generated by the powertrain [1–3]. Since the object of this research is the vibration degradation problem of the whole vehicle under idle conditions, this paper will focus on the vibration excitation generated by the powertrain during operation and the vibration conditions of key components in the vibration transmission link.

This paper takes a domestic brand SUV (referred to as Type A vehicle in the text) as the research object and selects a market-positioned comparable benchmark vehicle (Type B vehicle) for comparison, testing the vibration situation of several key points that may affect NVH under idle conditions. Based on market research feedback, vehicles of both types with less than 20,000 kilometers and high mileage of 50,000 to 100,000 kilometers were selected for research, to analyze the situation and reasons for NVH performance degradation.

2 Experimental Platform and Testing Method

In past research, designers often focused more on the NVH performance of new vehicles, using simulation and other methods to tune the vehicle to a relatively good state. However, it is difficult to completely solve NVH problems at the design stage. Errors introduced during design, manufacturing, and assembly could lead to issues. Testing prototype vehicles can solve some problems, but after a period of use, wear and aging of various components and connectors may lead to a decline in damping performance [4–6]. Therefore, this article focuses on the causes of the degradation of whole vehicle NVH performance.

As the power source of the car and being of significant mass, the engine is an important source of excitation. Vibrations generated at the engine are transmitted to the frame and body through the suspension system. Elastic rubber suspension components are important damping parts [7, 8] and must be included in the analysis of vibration transmission paths. For drivers and passengers, the direct impact of decreased damping performance on ride comfort is often manifested in obvious steering wheel and seat vibration, increased interior noise, etc. [9]. In addition, during the operation of the engine, vibrations and noise generated by the exhaust system and cooling system are also areas of concern [10], please refer to Figure 1 for the specific process.

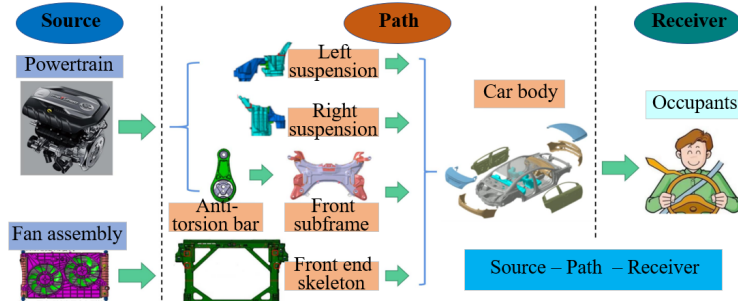


Figure 1. Transmission path diagram

The test location for this experiment is an automobile test field in China. Due to market research feedback indicating that this model experiences increased idle vibration after medium to long mileage, the test conditions were set to idle, with test statuses in parking gear(P)/reverse gear(R)/forward gear(D) and with air conditioning on/off (i.e., P_AC OFF, R_AC OFF, D_AC OFF, P_AC ON, R_AC ON, D_AC ON), see Table 1 for specific test information.

Since the tested vehicle uses an automatic transmission, to accurately analyze the driver's sensory characteristics in a ready-to-drive state, the transmission was forced to engage in 1st gear during D gear(forward gear) testing to prevent the transmission from automatically disengaging power when stopped.

Table 1. Test conditions

Test Conditions	Condition 1	Condition 2	Condition 3
Temperature	Normal temperature (Hot Engine)		
Test gear position	P	R	D
Air conditioning state	AC OFF	AC ON	
Sensor direction	X	Y	Z
Engine state	Idle steady state		
RPM	800 rpm		
Test duration per condition	30 seconds		
Data statistics information	Frequency	Amplitude	

In the test, acceleration sensors were placed at 17 points as shown in Table 2, using LMS's 32-channel data acquisition system to collect data. The data collected were then analyzed and processed using the Signature Testing-Advanced module in LMS Test Lab.

Photos of sensor placements at several important points are shown in Figure 2.

The basic parameters of the three vehicles tested are shown in Table 3.

Table 2. Acceleration sensor locations

Acceleration Sensor Locations	
Active end of left engine mount - Engine	Passive end of left engine mount - Frame
Active end of right engine mount - Engine	Passive end of right engine mount - Frame
Active end of rear engine mount - Engine	Passive end of rear engine mount - Frame
Top end of left front shock absorber	Bottom end of left front shock absorber
Top end of right front shock absorber	Bottom end of right front shock absorber
Active end of radiator vibration isolation pad - Radiator	Passive end of radiator vibration isolation pad - Frame
Fan	Seat rail
Steering wheel	



Figure 2. Selected sensor locations on the vehicle

Table 3. Acceleration sensor locations

Parameter \ Type	Type	Type A Vehicle	Type B Vehicle
Category	Mid-size SUV	Mid-sizeSUV	
Energy type	Gasoline	Gasoline	
Dimensions (LWH) (mm)	4740*1910*1775	4858*1942*1670	
Curb weight (kg)	1749	1708	
Engine	2.0T 252 HP L4	1.5T 193 HP L4	
Displacement (mL)	1991	1498	

3 Analysis of Driver's Sensory Characteristics

First, two points that have the most direct and strongest impact on the driver's sensation were analyzed: the steering wheel and seat rail.

3.1 Steering Wheel and Seat Rail

3.1.1 Characteristics of vibration acceleration change

The larger the vibration acceleration, the worse the NVH performance [10–12]. In this test, the vibration acceleration magnitude in XYZ three directions for each point was obtained through data acquisition, measured in g. The XYZ three directions are unified with the vehicle's orientation, i.e., the X direction is directly in front of the driver's seat, the Y direction is to the left of the driver's seat, and the Z direction is directly above the driver's seat, as shown in Figure 3.

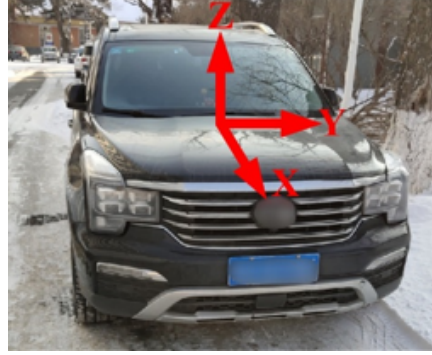


Figure 3. Schematic of automobile coordinate system

To comprehensively compare the vibration acceleration magnitude under various conditions for each vehicle, vibration acceleration S (m/s^2) is calculated as in Eq. (1) [13, 14]:

$$S = \sqrt{9.8^2 * (a_x^2 + a_y^2 + a_z^2)} \quad (1)$$

where, S is the vibration acceleration at that point (m/s^2); a_x is the vibration acceleration in the X direction at that point (m/s^2); a_y is the vibration acceleration in the Y direction at that point (m/s^2); a_z is the vibration acceleration in the Z direction at that point (m/s^2).

The changes in vibration acceleration for the steering wheel and seat rail under various conditions are shown in Figures 4 and 5, where the new car data for Vehicle A is the original factory test data from the car manufacture.

As can be seen from Figure 4, with the increase in mileage, the vibration acceleration at the steering wheel measurement point of both Vehicle types A and B gradually increases, with Vehicle B's increase slightly less than Vehicle A; Vehicle A shows a significant increase in vibration acceleration at the R gear position of the steering wheel measurement point, with smaller changes in other gear positions. The vibration acceleration with the air conditioning on is significantly higher than when it is off.

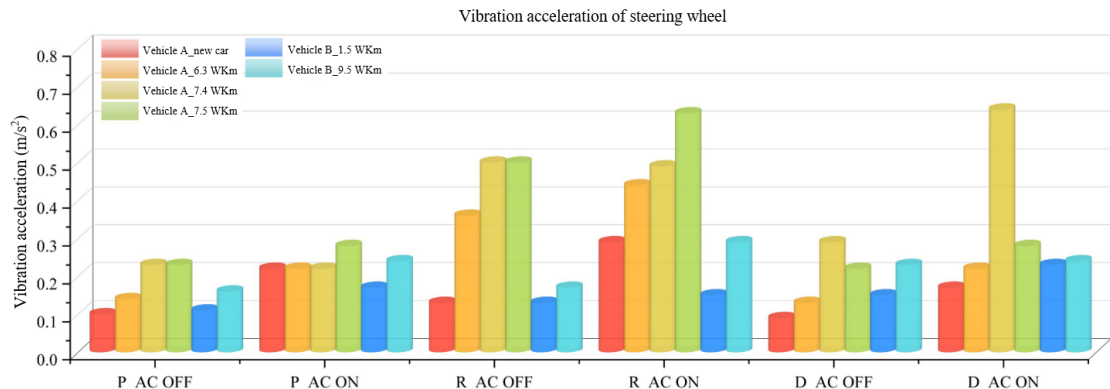


Figure 4. Vibration acceleration of steering wheel

As can be seen from Figures 4 and 5, with the increase in driving mileage, the vibration acceleration at both measurement points for Vehicles A and B gradually increases, with Vehicle B's increase slightly smaller than Vehicle A. Vehicle A shows a significant increase in vibration acceleration at the R gear position at the steering wheel measurement point, with smaller changes in other gear positions. The vibration acceleration with the air conditioning on is significantly greater than when it is off.

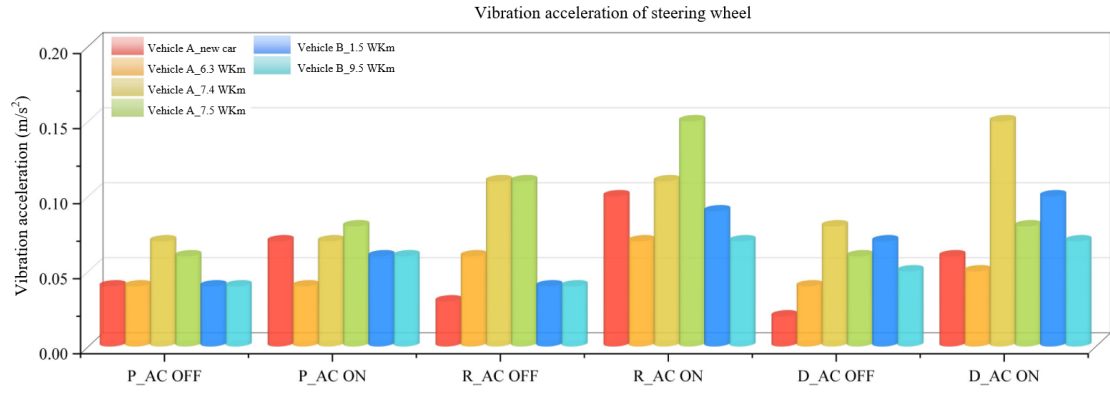


Figure 5. Seat rail vibration acceleration

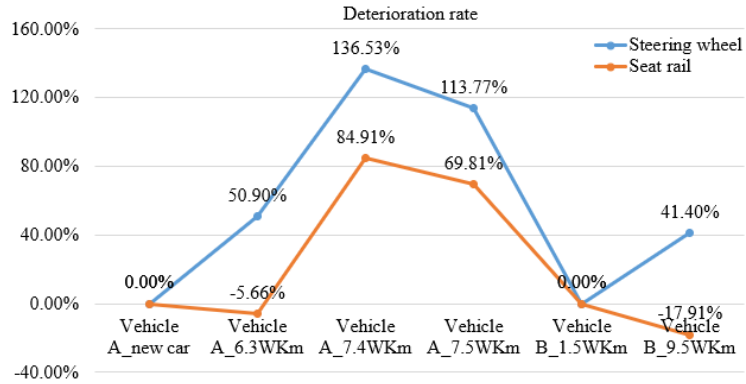


Figure 6. Trend of driver's sensory changes

As shown in Figure 6, by taking the average vibration value of each gear position for each vehicle and comparing the high mileage vehicles with the new car (Vehicle B model at 1.5 WKm), the changes in vibration amplitude at the two points can be seen more clearly.

The steering wheel and seat rail are the two most directly perceptible test points for occupants, reflecting the overall NVH performance of the vehicle. Therefore, to further investigate the source of the vibration, this study will analyze the vibration frequency of the two points.

3.1.2 Vibration frequency domain analysis

To explore the source of vibration excitation, we collected frequency domain data for vibrations at each point. The data were processed, marking the frequency of the highest vibration within 100Hz, as shown in Figure 7.

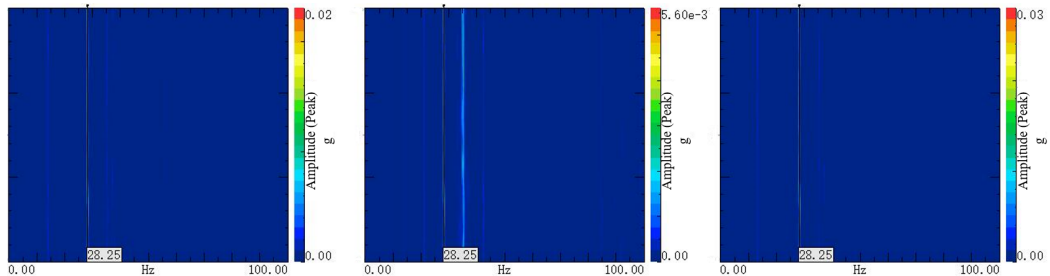


Figure 7. Vibration frequency domain analysis diagram

Note: Steering Wheel +X+Y+Z P Gear AC off (Sensor at steering wheel position, sensor X direction as the vehicle's +X direction, sensor Y direction as the vehicle's +Y direction, sensor Z direction as the vehicle's +Z direction, P gear, air conditioning system off)

This study mainly focuses on the deterioration of whole vehicle NVH performance with increased driving mileage and does not consider the direction of vibration as a major concern. Therefore, the vibration signals collected under idle conditions are subjected to Fourier transform. Using the spectrum analysis method [15], we analyze the changes in amplitude of vibrations at the steering wheel and seat rail in different frequencies under different gear positions and air conditioning on/off states, as shown in Figures 8 and 9.

The vibration acceleration frequency spectrum analysis results of the steering wheel position are shown in Figure 8. It can be observed that under idle conditions, the frequencies with larger amplitudes are around 27 Hz and 42 Hz. The amplitude within this range shows a trend of being smallest in P gear and largest in R gear, with the amplitude slightly greater when the air conditioning is on compared to when it is off. The vibration acceleration frequency spectrum analysis results at the seat rail are shown in Figure 9. It can be seen that the frequency spectrum distribution is similar to that at the steering wheel, but with a smaller amplitude. The amplitude is generally smallest in P gear and largest in D gear.

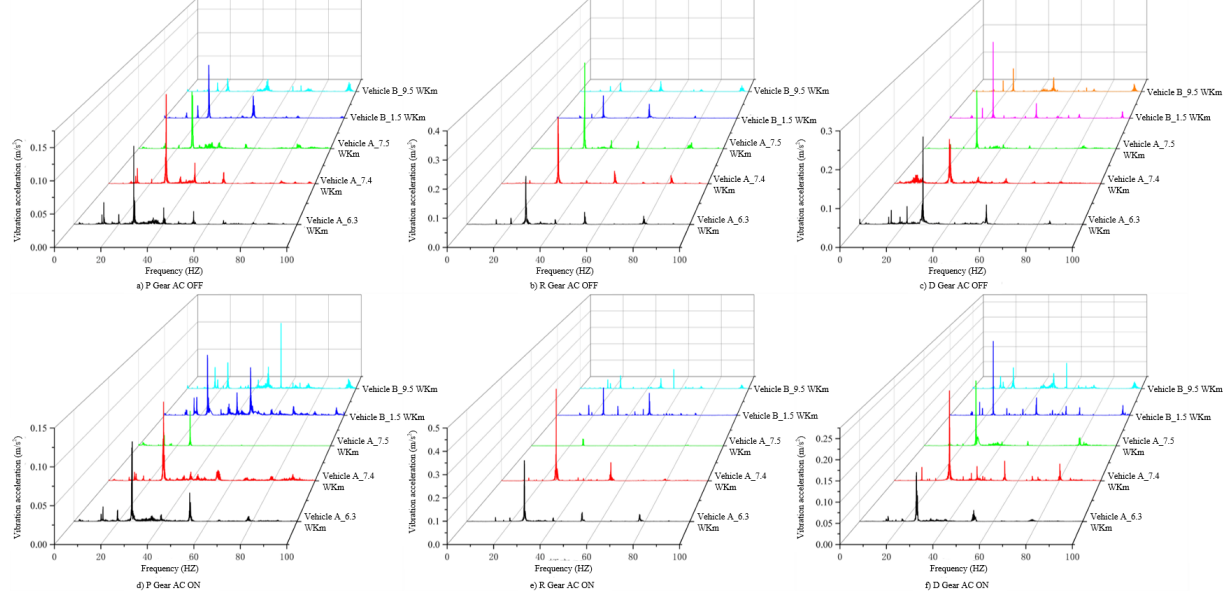


Figure 8. Steering wheel frequency spectrum

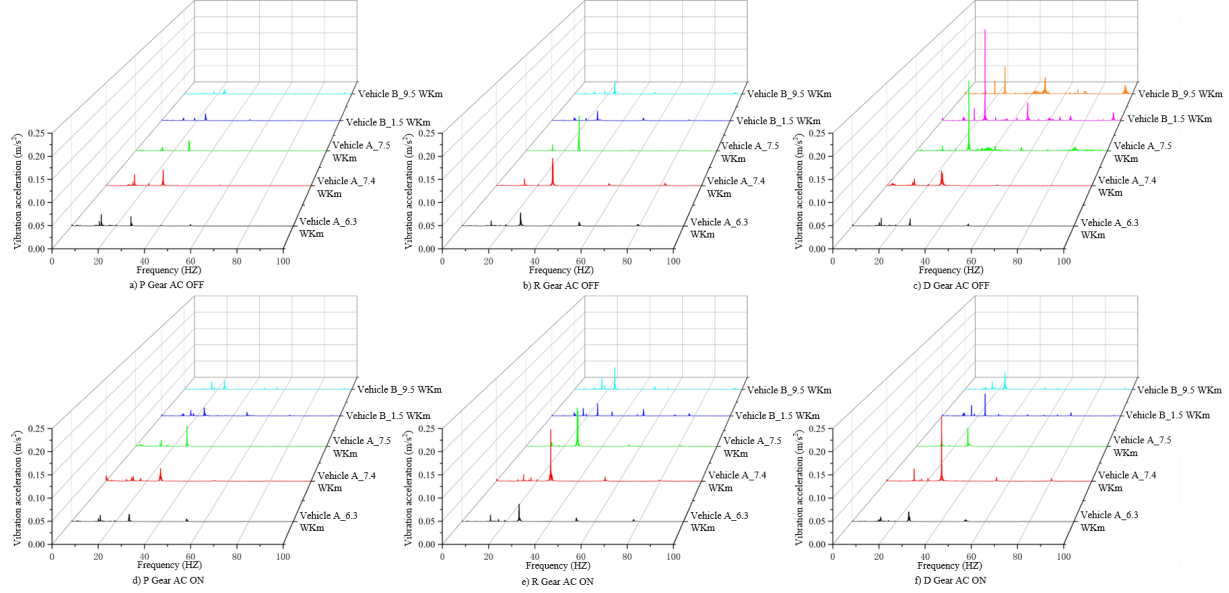


Figure 9. Seat rail frequency spectrum

Both vehicle models have an engine idle speed of 800 rpm, corresponding to a 2nd order engine vibration frequency of around 27 Hz. This indicates that the main source of vehicle vibration is the powertrain. Therefore, the next focus is the vibration magnitude and vibration isolation rate at the engine mounts.

4 Powertrain Vibration Isolation Characteristics Analysis

The suspension system serves as a connector between the powertrain and the body of the vehicle. Its main functions are to support the powertrain, reduce the impact of vibrations emanating from the powertrain on the whole

vehicle, and limit the amount of powertrain jitter. It is a key guarantee for improving the overall NVH performance of the vehicle. Both vehicle models selected in this study use a three-point rubber suspension system, which compared to hydraulic suspensions, has the advantages of a simpler structure, better cost-effectiveness, easier maintenance, and a longer lifespan [16, 17]. The failure of rubber suspensions is mainly caused by fatigue damage to the rubber parts [8]. To ensure the rubber suspension maintains a stable vibration isolation effect over a long period, it is necessary to prevent it from failing during this time.

As known from the frequency spectrum analysis of the steering wheel and seat rail in section 3.1.2, the main source of vibration is the 2nd order vibration of the four-cylinder engine of the car. Therefore, the next section will next focus on the analysis of test data at the active and passive ends of the three suspension points. The active end refers to the side of the suspension connected to the engine, and the passive end is the side connected to the frame, with a rubber isolation block between the active and passive ends.

4.1 Vibration Acceleration Change Characteristics

Figures 10-12 show the comparison of vibration acceleration for the left, right, and rear suspensions respectively. It can be observed that as the mileage increases, the vibration magnitude at the active ends of each suspension point for both vehicle models increases. Therefore, it is believed that a significant reason for the decline in whole vehicle NVH performance is the intensification of engine vibration itself [18]. Analysis of the passive end data shows that the vibration magnitude at the passive end of Vehicle A is consistent with the trend at the active end, while Vehicle B maintains better passive end vibration relative to Vehicle A. It is speculated that the degradation of the rubber suspension in Vehicle A is greater than in Vehicle B. The following section will compare and analyze the isolation rates at each point.

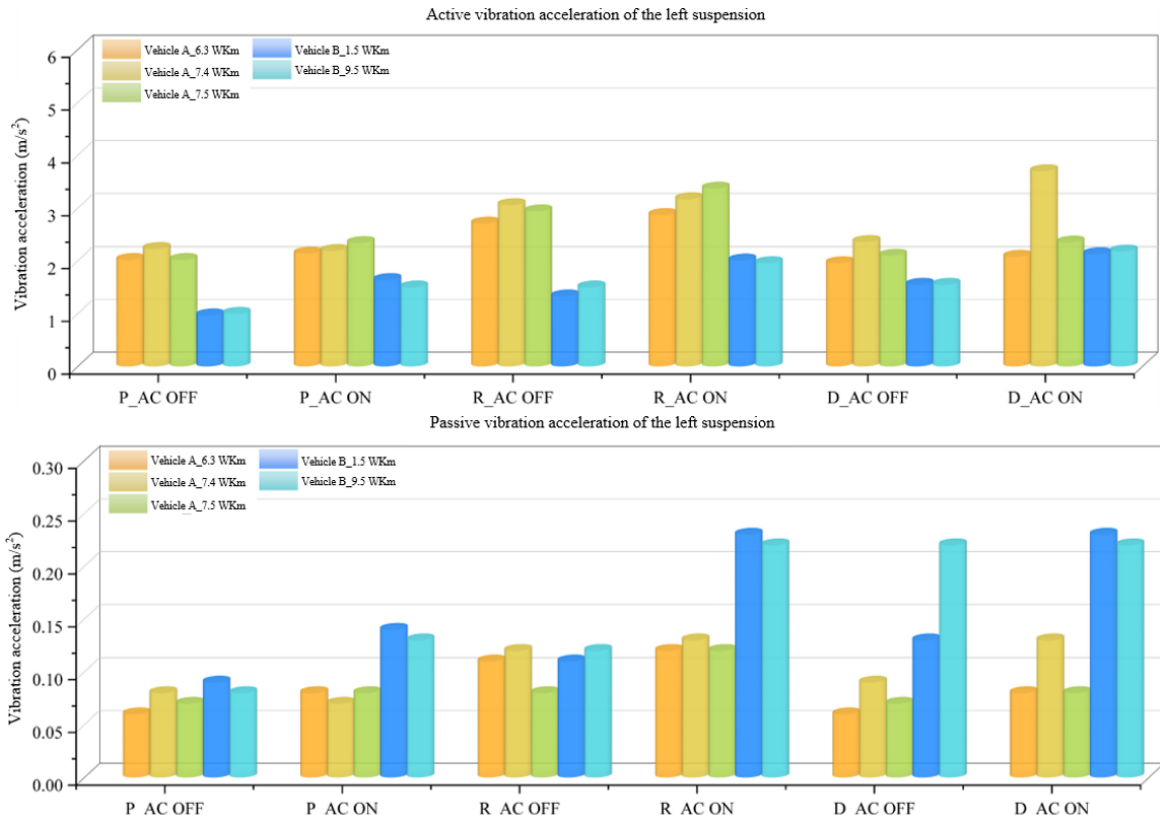


Figure 10. Vibration acceleration of the left suspension

4.2 Comparative Analysis of Vibration Isolation Rate

The formula for calculating the vibration isolation rate of the powertrain suspension system is [19]:

$$T = 20 \lg (a^e / a^c) \quad (2)$$

where, T is the suspension vibration isolation rate (dB); a^e is the vibration acceleration at the active end of the suspension (m/s^2); a^c is the vibration acceleration at the passive end of the suspension (m/s^2).

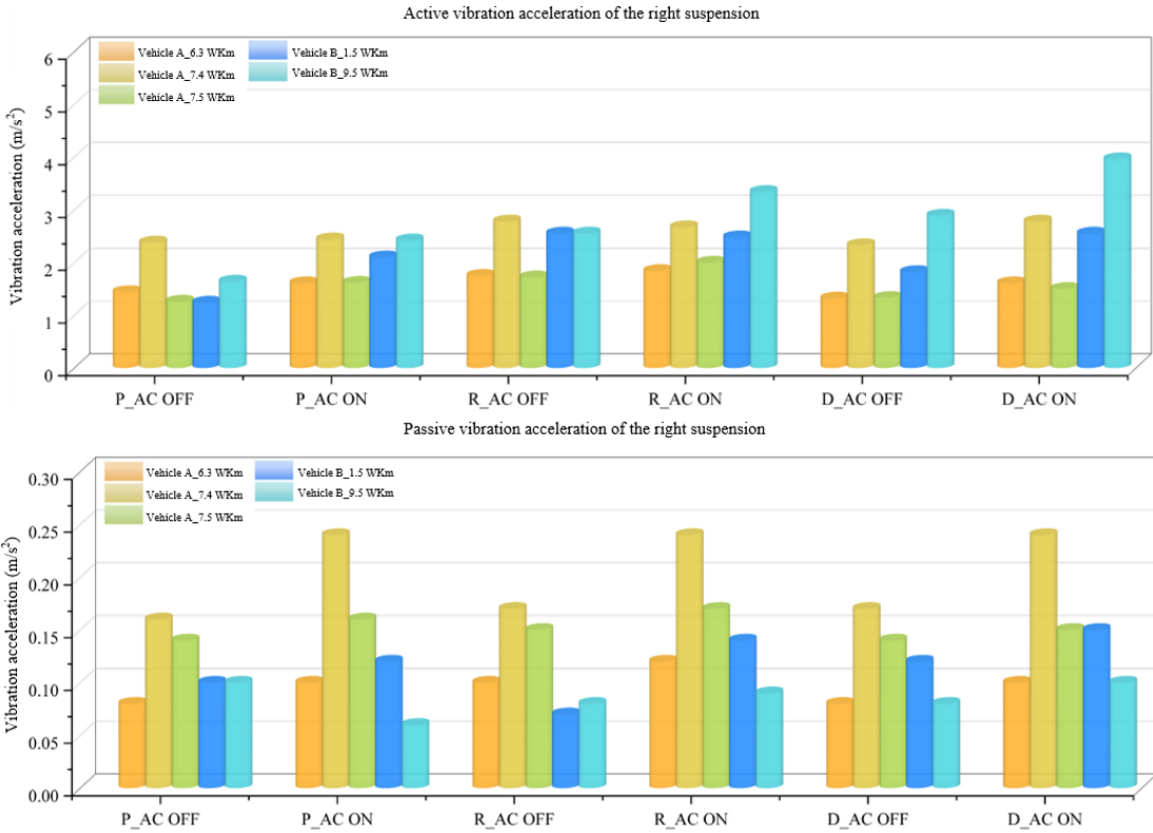


Figure 11. Vibration acceleration of the right suspension

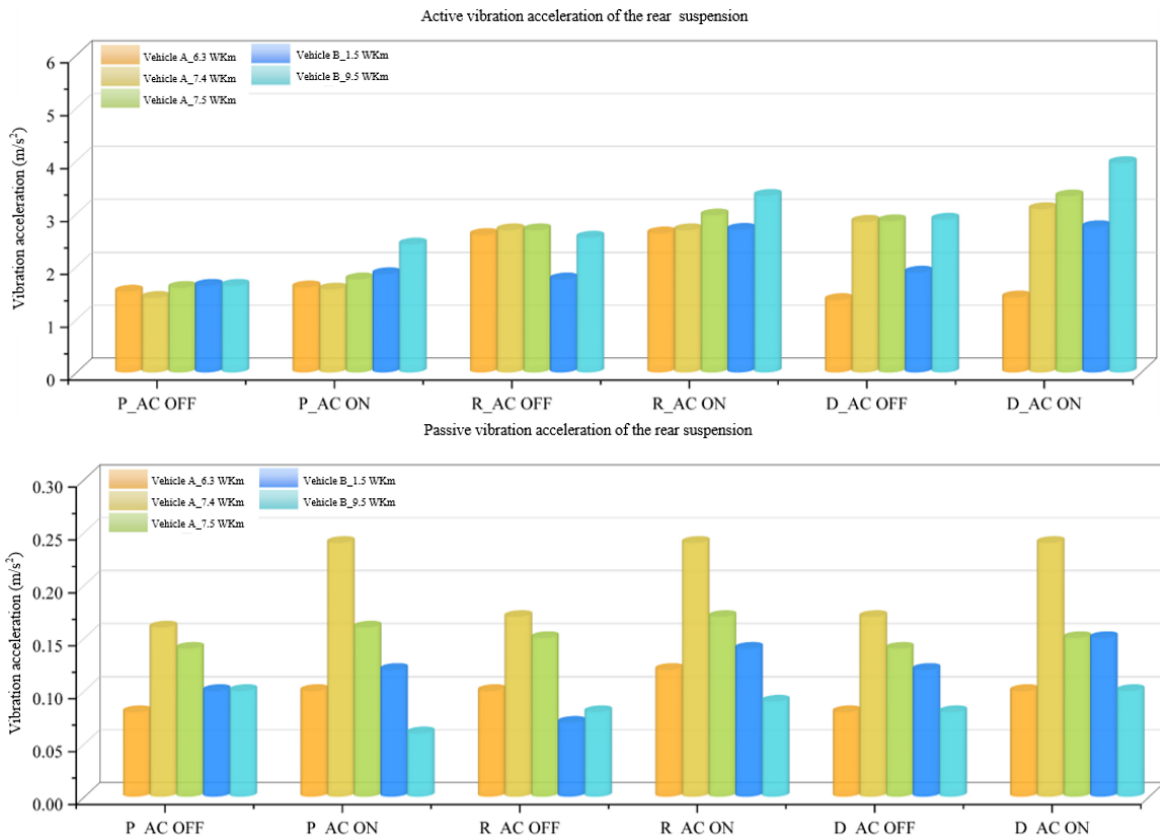


Figure 12. Vibration acceleration of the rear suspension

Analysis from Figures 13-15 shows that the suspension vibration isolation performance of Vehicle B does not significantly degrade. Despite the increase in engine vibration due to higher mileage, the isolation rate of Vehicle B at 9.5 WKm even shows an increase. In contrast, Vehicle A exhibits a decrease in suspension isolation rate, especially noticeable in the right suspension.

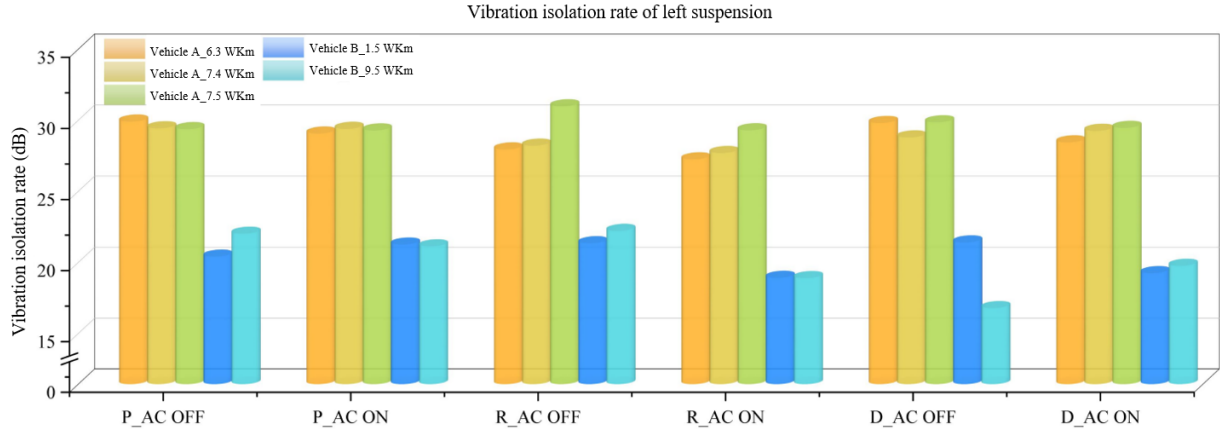


Figure 13. Vibration isolation rate of left suspension

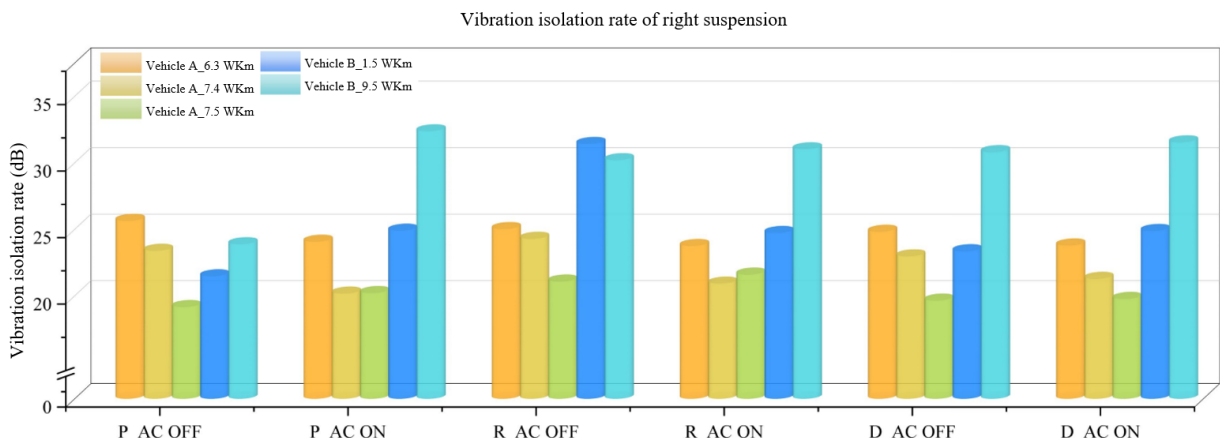


Figure 14. Vibration isolation rate of right suspension

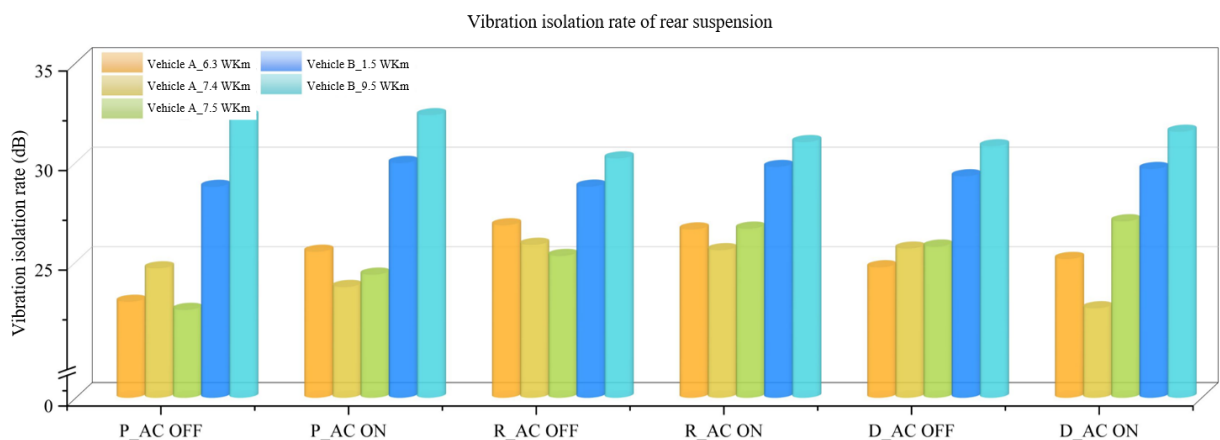


Figure 15. Vibration isolation rate of rear suspension

5 NVH Performance Degradation Cause Verification

5.1 Vibration Acceleration Change Characteristics

To further explore the impact of suspension changes on the NVH performance of Vehicle A, we selected a 7.4 WKm Vehicle A for follow-up testing. The vehicle was retested at 8.9 WKm after reaching this mileage, and the change in overall NVH performance was compared and analyzed by replacing the old suspension with a new one. The vibration comparison at the steering wheel and seat rail when using the old and new suspensions is shown in Figures 16 and 17.

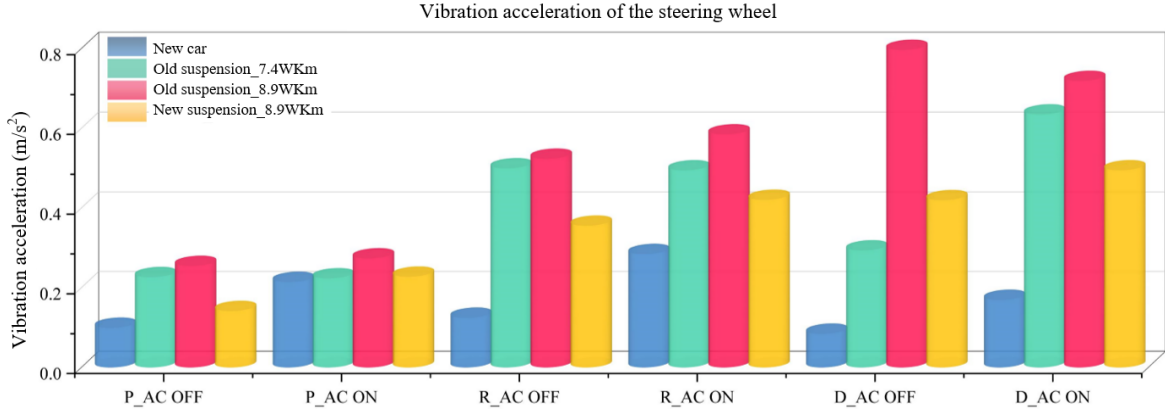


Figure 16. Vibration acceleration of the steering wheel

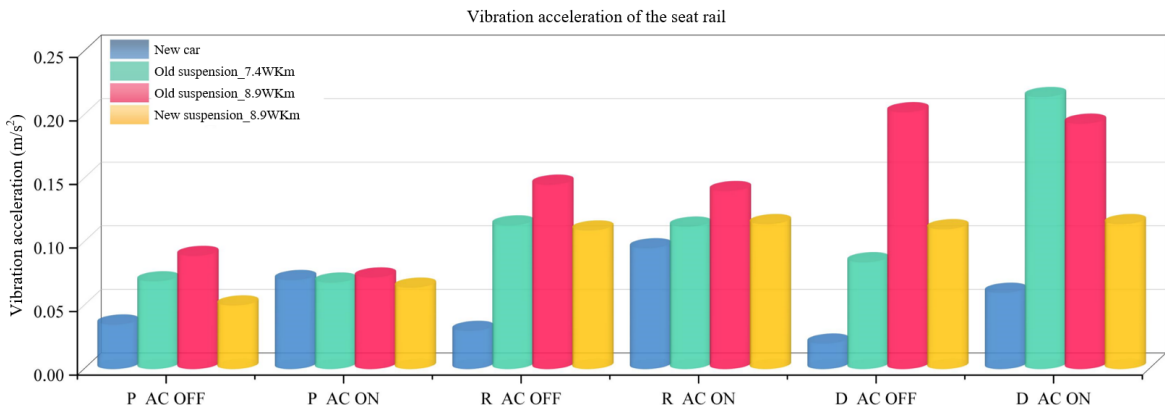


Figure 17. Vibration acceleration of the seat rail

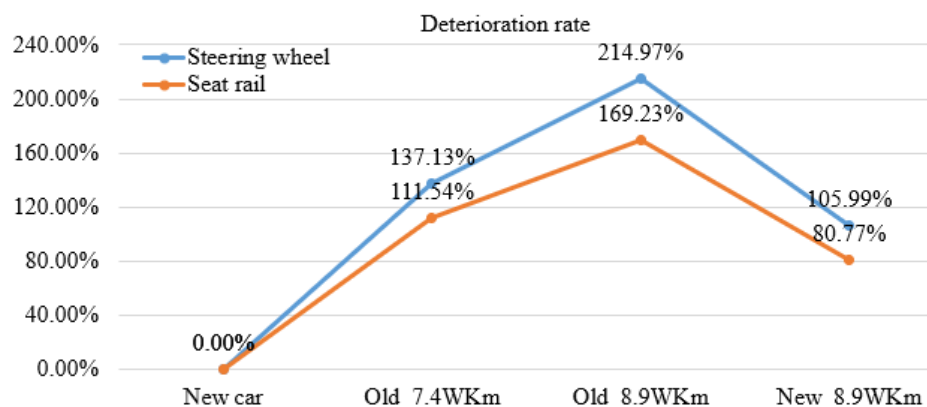


Figure 18. Trend of driver's sensory changes

As can be seen from Figures 16 and 17, under P gear, the vibration condition at the steering wheel changes little. After replacing with new suspension at 8.9 WKm, the vibration acceleration values are close to the original factory

data. However, the changes in R and D gears are more significant, consistent with the previous text. When using the old suspension, the vibration acceleration at 8.9 WKm is slightly higher than at 7.4 WKm, but significantly decreases after replacing with the new suspension.

Figure 18 shows the deterioration comparison of the steering wheel and seat rail when using the old and new suspensions.

5.2 Suspension Vibration Isolation Analysis

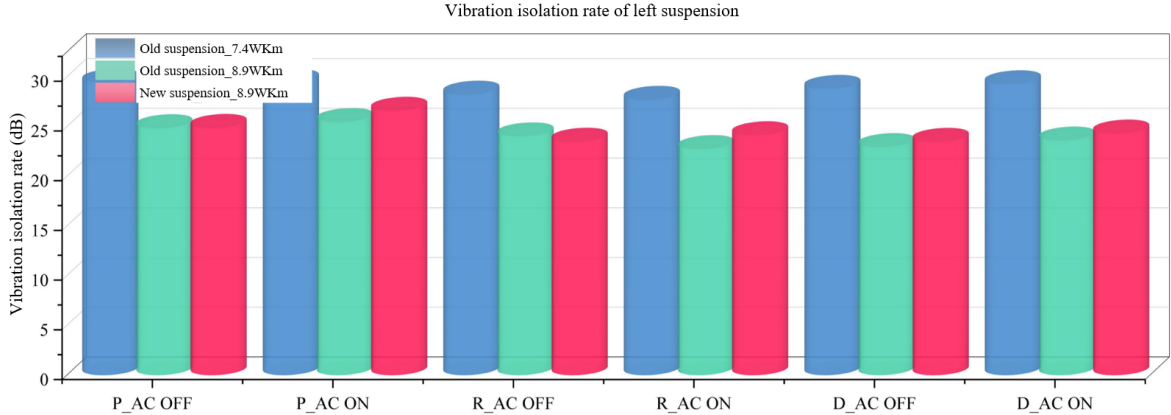


Figure 19. Left suspension vibration isolation rate

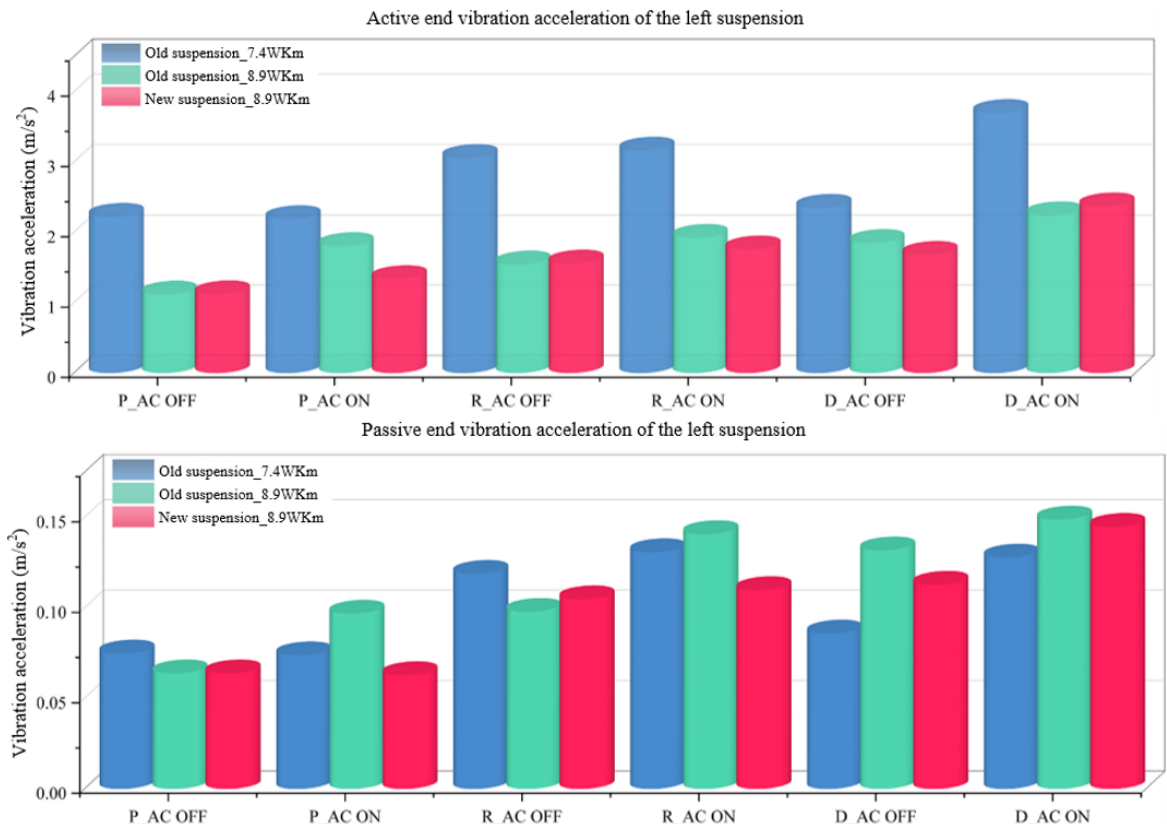


Figure 20. Active and passive end vibration accelerations of the left suspension

Similarly, we further analyze the data for each suspension point.

As shown in Figures 19 and 20, at the left suspension point, when using the old suspension, although the active end amplitude is clearly larger at 7.4 WKm than at 8.9 WKm, the passive end amplitude data at 8.9 WKm is slightly larger than at 7.4 WKm, and the isolation rate is also higher at 7.4 WKm than at 8.9 WKm. This indicates that the vibration isolation performance of the left suspension has already declined. After replacing with new suspension,

the isolation rate slightly increases, but since the active end amplitude is much lower than the 7.4 WKm state with old suspension, the isolation rate does not exceed it. However, the amplitude at the passive end is smaller with the new suspension.

As shown in Figures 21 and 22, at the right suspension point, there is not much difference in the isolation rates between the three conditions. In terms of vibration, with the old suspension, the active end vibration acceleration at 8.9 WKm is greater than at 7.4 WKm, but the passive end values are close. After replacing with new suspension, vibration at both the active and passive ends significantly decreases, and the isolation rate is the best.

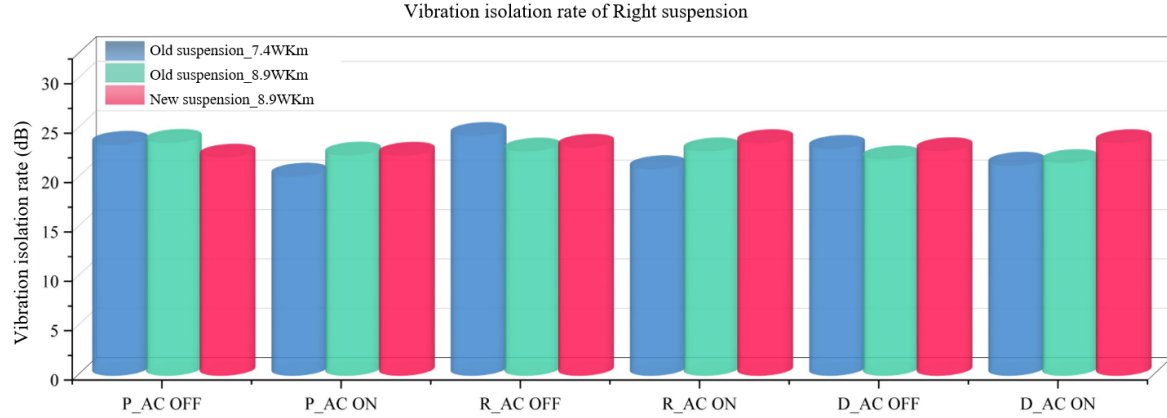


Figure 21. Right suspension vibration isolation rate

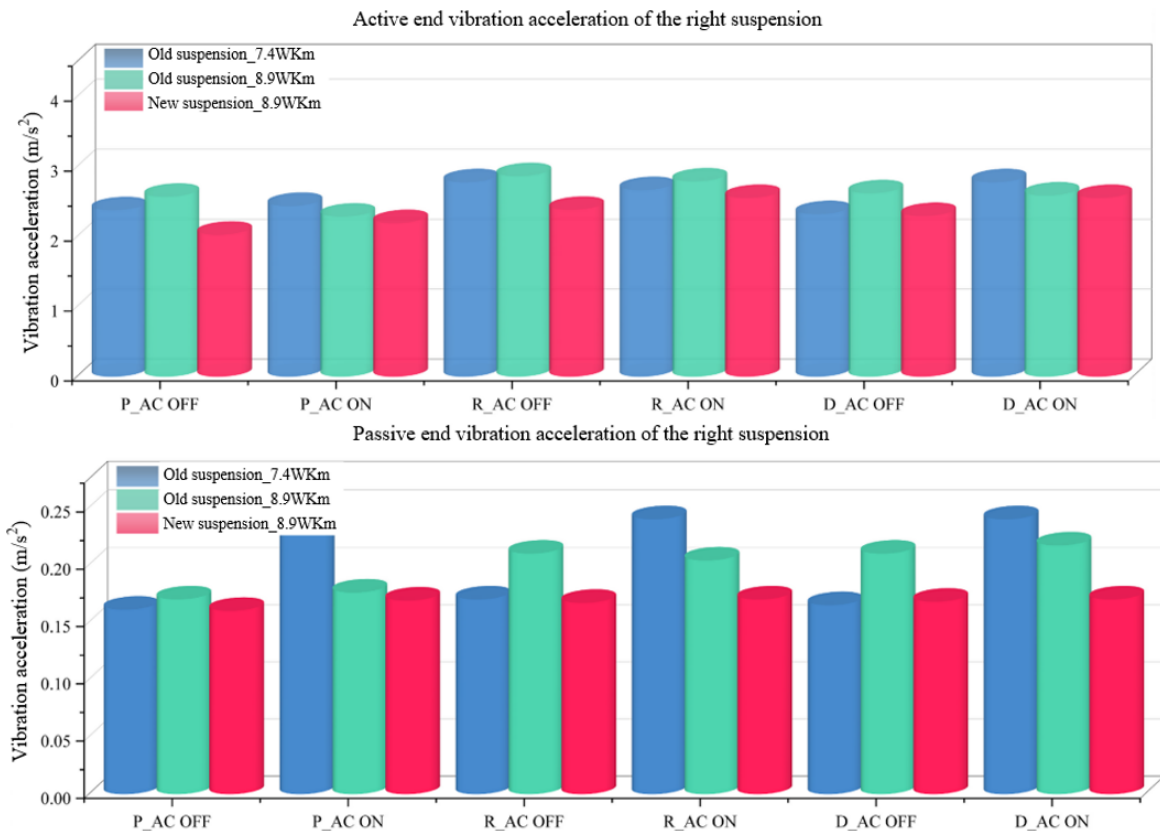


Figure 22. Active and passive end vibration accelerations of the right suspension

As seen in Figures 23 and 24, at the rear suspension point, the old suspension isolation rate at 8.9 WKm is higher than at 7.4 WKm, but still, the new suspension offers the best isolation rate. Analyzing the vibration at the active and passive ends reveals that, with the old suspension, the active end vibration at 8.9 WKm is greater than at 7.4 WKm. Although the isolation rate is better, the passive end vibration is still high. After replacing with new suspension, vibration at both the active and passive ends decreases.

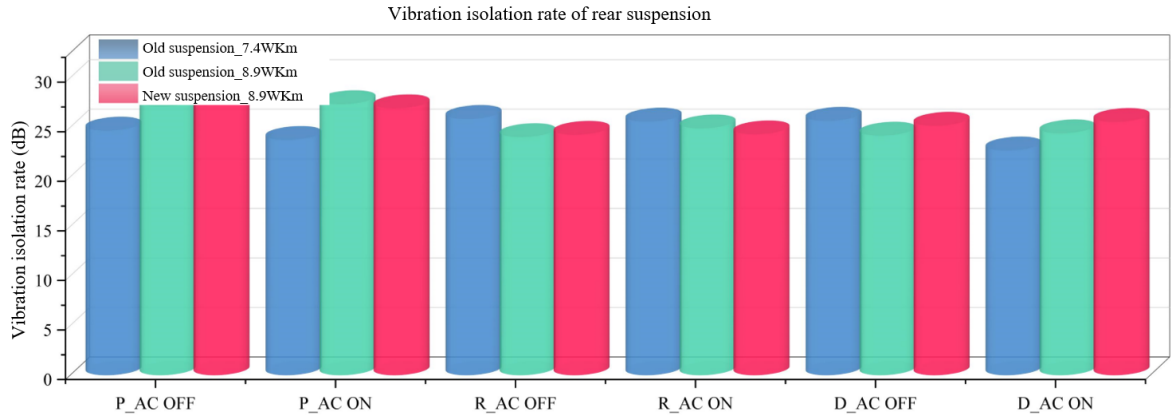


Figure 23. Vibration isolation rate of rear suspension

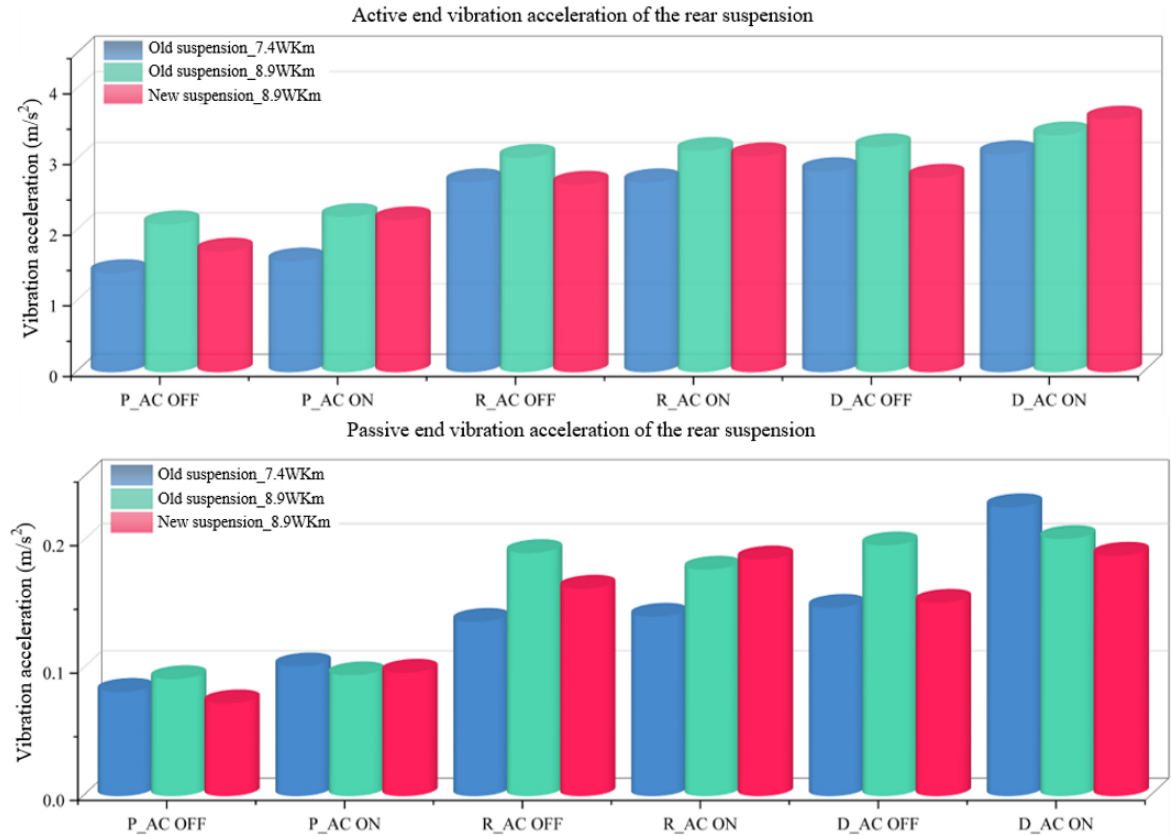


Figure 24. Active and passive end vibration accelerations of the rear suspension

This paper summarizes the comparison of the average values of isolation rates and vibration at each suspension point when using old and new suspensions, as shown in Figure 25. It can be concluded that with the increase in vehicle mileage, the suspension isolation rate does not significantly decrease and may even increase due to the increase in active end vibration. However, after replacing with new suspension, there is a significant decrease in active end vibration, and the isolation rate is also better.

6 Conclusions

This paper mainly conducts vibration tests under idle conditions on a certain SUV and its benchmark vehicle, obtaining the characteristics of vibration changes at the steering wheel and seat rail under low and high mileage conditions. It also measures the vibration acceleration at the left, right, and rear suspension points to explore the reasons for the deterioration of the vehicle's NVH performance. The following conclusions are drawn:

- (1) By comparing and analyzing the changes in vibration acceleration at the steering wheel and seat rail, it is evident that the vehicle's NVH performance decreases with increased mileage, especially noticeable in D gear.

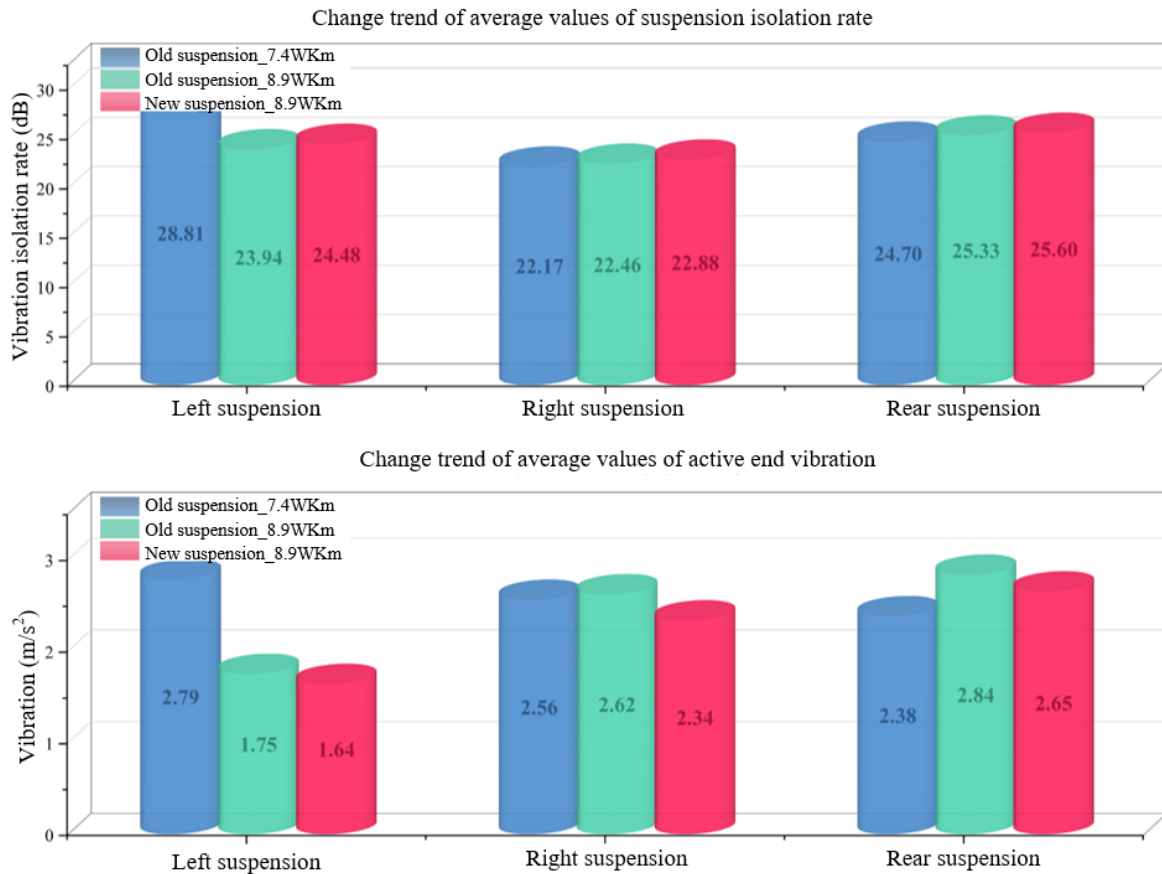


Figure 25. Change trends of average values of isolation rates and vibrations of suspensions

(2) Analysis of the vibration spectrum graphs of the steering wheel and seat rail shows that the largest vibration frequencies are around 27 Hz and 24 Hz. Since the test vehicles all have four-cylinder engines, the main source of vehicle vibration is the 2nd order vibration of the engine.

(3) Through follow-up tests on the same vehicle and tests with new suspension replacements, it is concluded that the deterioration of the vehicle's NVH performance is due to two factors: increased engine vibration and degradation of rubber suspension performance.

(4) Since a car is a multi-mass vibration system and the suspension does not exhibit significant damage after high mileage use, if the active end vibration is not particularly large, the degradation of the rubber suspension's performance is more reflected in the changes in active end vibration.

Therefore, for whole vehicle manufacturers, at the beginning of designing a new vehicle, to improve user experience and ensure good NVH performance even at high mileage, the following approaches can be considered:

(1) Since the main excitation source is the 2nd order vibration of the engine, vibrations near the engine should avoid this frequency range as much as possible.

(2) Optimize the vibration isolation and durability performance of the suspension rubber blocks to prevent performance degradation over long-term use.

(3) Optimize the stiffness ratio of the rubber blocks at the three suspension points, leaving appropriate room for suspension performance degradation, so that even if one or two suspensions slightly degrade, they can still ensure the combined vibration isolation performance of all three.

Data Availability

The data used to support the findings of this study are available from the corresponding author upon request.

Conflict of Interest

The authors declare that they have no conflicts of interest.

References

- [1] H. Zhou, H. Liu, P. Gao, and C. L. Xiang, “Optimization design and performance analysis of vehicle powertrain mounting system,” *Chin. J. Mech. Eng.*, vol. 31, p. 31, 2018. <https://doi.org/10.1186/s10033-018-0237-2>
- [2] H. Lü, Z. Zheng, X. Huang, W. B. Shangguan, and K. Zhao, “Uncertainty propagation analysis of fuzzy uncertain structures involving imprecise membership functions,” *Int. J. Comput. Methods*, vol. 20, no. 1, p. 2250036, 2023. <https://doi.org/10.1142/S0219876222500360>
- [3] B. Cai, W. B. Shangguan, and H. Lü, “An efficient analysis and optimization method for powertrain mounting systems involving interval uncertainty,” *Proc. Inst. Mech. Eng. Part D: J. Automob. Eng.*, vol. 234, no. 5, pp. 1318–1329, 2020. <https://doi.org/10.1177/0954407019880370>
- [4] H. Lü, H. Mao, X. Huang, H. Yin, and W. B. Shangguan, “An effective approach for reliability-based robust design optimization of uncertain powertrain mounting systems involving imprecise information,” *Eng. Comput.*, vol. 38, pp. 1193–1214, 2021. <https://doi.org/10.1007/s00366-020-01266-7>
- [5] H. Lü, K. Yang, X. Huang, W. B. Shangguan, and K. Zhao, “Uncertainty and correlation propagation analysis of powertrain mounting systems based on multi-ellipsoid convex model,” *Mech. Syst. Signal Process.*, vol. 173, p. 109058, 2022. <https://doi.org/10.1016/j.ymssp.2022.109058>
- [6] G. Liu, R. Luo, and S. Liu, “A new interval multi-objective optimization method for uncertain problems with dependent interval variables,” *Int. J. Comput. Methods*, vol. 17, no. 10, p. 2050007, 2020. <https://doi.org/10.142/S0219876220500073>
- [7] B. Angrosch, M. Plöchl, and W. Reinalter, “Mode decoupling concepts of an engine mount system for practical application,” *Proc. Inst. Mech. Eng. Part K J. Multi-body Dyn.*, vol. 229, no. 4, pp. 331–343, 2015. <https://doi.org/10.1177/1464419314564020>
- [8] I. L. Ladipo, J. D. Fadly, and W. F. Faris, “Characterization of magnetorheological elastomer (MRE) engine mounts,” *Mater. Today Proc.*, vol. 3, no. 2, pp. 411–418, 2016. <https://doi.org/10.1016/j.matpr.2016.01.029>
- [9] L. Wang, C. Xiong, X. Wang, M. Xu, and Y. Li, “A dimension-wise method and its improvement for multidisciplinary interval uncertainty analysis,” *Appl. Math. Modell.*, vol. 59, pp. 680–695, 2018. <https://doi.org/10.1016/j.apm.2018.02.022>
- [10] L. K. Yang, H. Y. Li, M. Ahmadian, and B. Ma, “Analysis of the influence of engine torque excitation on clutch judder,” *J. Vib. Control*, vol. 23, no. 4, pp. 645–655, 2017. <https://doi.org/10.1177/1077546315582291>
- [11] H. Rahnejat, S. Theodossiades, P. Kelly, and M. T. Menday, “Drivetrain noise, vibration, and harshness,” *Encycl. Automot. Eng.*, vol. 17, pp. 1–13, 2014. <https://doi.org/10.1002/9781118354179.auto096>
- [12] M. Menday and M. Ebrahimi, “The application of dynamic modelling using parametric design methods for an automotive driveline system,” in *Multi-body Dynamics Monitoring and Simulation Techniques Conference*, 1997, pp. 67–79.
- [13] R. Turnbull, O. R. Miknas, M. Mohammadpour, and H. Rahnejat, “Combined experimental and flexible multi-body dynamic investigation of high-energy impact-induced driveline vibration,” *Proc. Inst. Mech. Eng. Part K J. Multi-body Dyn.*, vol. 231, no. 1, pp. 181–193, 2017. <https://doi.org/10.1177/1464419316659996>
- [14] S. Theodossiades, M. Gnanakumarr, H. Rahnejat, and M. Menday, “Mode identification in impact-induced high-frequency vehicular driveline vibrations using an elasto-multi-body dynamics approach,” *Proc. Inst. Mech. Eng. Part K J. Multi-body Dyn.*, vol. 218, no. 2, pp. 81–94, 2004. <https://doi.org/10.1243/146441904323074549>
- [15] Y. Wang, X. Li, G. Qiao, and T. Lim, “Effect of component flexibility on axle system dynamics,” *SAE Int. J. Veh. Dyn., Stab. NVH*, vol. 1, no. 2, pp. 400–407, 2017. <https://doi.org/10.4271/2017-01-1772>
- [16] Y. H. Zweiri, J. F. Whidborne, and L. D. Seneviratne, “Dynamic simulation of a single-cylinder diesel engine including dynamometer modelling and friction,” *Proc. Inst. Mech. Eng., Part D: J. Automob. Eng.*, vol. 213, no. 4, pp. 391–402, 1999. <https://doi.org/10.1243/0954407991526955>
- [17] P. R. Hooper, “Low noise, vibration and harshness solutions for in-line three-cylinder range extender and hybrid electric vehicles,” *Int. J. Engine Res.*, vol. 22, no. 2, pp. 581–591, 2021. <https://doi.org/10.1177/1468087419859084>
- [18] P. Shital, C. Ghosh, H. Talwar, A. Gosain, and P. S. Dayal, “A study of engine mount optimisation of three-cylinder engine through multi-body dynamic simulation and its verification by vehicle measurement,” *SAE Tech. Pap.*, no. 2015-26-0126, 2015. <https://doi.org/10.4271/2015-26-0126>
- [19] K. Torii and K. Noumura, “Sound quality evaluation method for engine combustion noise with consideration of perceived fluctuation (first report),” *Trans. Soc. Automot. Eng. Jpn.*, vol. 49, no. 4, pp. 367–374, 2018. <https://doi.org/10.11351/jsaeronbun.49.772>